

Activation Functions Considered Harmful: Recovering Neural Network Weights through Controlled Channels

Jesse Spielman David Oswald Mark Ryan Jo Van Bulck
School of Computer Science School of Computer Science School of Computer Science DistriNet
University of Birmingham University of Birmingham University of Birmingham KU Leuven, Belgium
Birmingham, UK Birmingham, UK Birmingham, UK Leuven, Belgium
jxs1366@student.bham.ac.uk d.f.oswald@bham.ac.uk m.d.ryan@bham.ac.uk jo.vanbulck@cs.kuleuven.be

Abstract—With high-stakes machine learning applications increasingly moving to untrusted end-user or cloud environments, safeguarding pre-trained model parameters becomes essential for protecting intellectual property and user privacy. Recent advancements in hardware-isolated enclaves, notably Intel SGX, hold the promise to secure the internal state of machine learning applications even against compromised operating systems. However, we show that privileged software adversaries can exploit input-dependent memory access patterns in common neural network activation functions to extract secret weights and biases from an SGX enclave. Our attack leverages the SGX-Step framework to obtain a noise-free, instruction-granular page-access trace. In a case study of an 11-input regression network using the Tensorflow Microlite library, we demonstrate complete recovery of all first-layer weights and biases, as well as partial recovery of parameters from deeper layers under specific conditions. Our novel attack technique requires only 20 queries per input per weight to obtain all first-layer weights and biases with an average absolute error of less than 1%, improving over prior model stealing attacks.

Additionally, a broader ecosystem analysis reveals the widespread use of activation functions with input-dependent memory access patterns in popular machine learning frameworks (either directly or via underlying math libraries). Our findings highlight the limitations of deploying confidential models in SGX enclaves and emphasise the need for stricter side-channel validation of machine learning implementations, akin to the vetting efforts applied to secure cryptographic libraries.

Index Terms—Machine Learning Security, Side Channel Attacks, Trusted Execution, Confidential Computing, SGX

1. Introduction

Training and deploying Machine Learning (ML) models, in particular neural networks, often requires a massive investment in computational resources. Hence, the threat of model stealing attacks is significant, because they allow an attacker to abscond with an ML application, causing substantial financial damage as well as security and privacy risks. Attacks could be used for industrial espionage (in the case of a network that solves a difficult problem, e.g., a sophisticated automated trading system), or to ease the creation of adversarial examples to defeat a

classification system, e.g., for spam filtering or intrusion detection. An application that incurs a fee to access per interaction could also be duplicated to remove this restriction. While existing model stealing attacks show how to duplicate neural networks essentially via brute force, they scale poorly for increasingly complex networks and require detailed access to output probabilities or physical access for measurements such as power consumption.

Because ML (both training and inference) requires substantial computation, there is a strong focus on performance. Further, because of the hardware requirements of ML training and inference (such as in the case of an AI model which backs an end user-accessible web interface), there is an increasing need to host ML workloads in the cloud, e.g., for scaling or to use the latest CPU and Graphics Processing Unit (GPU) hardware. However, this move off-premises and onto (often shared) hardware introduces a number of security concerns. To mitigate the risk, substantial work has been done using Trusted Execution Environments (TEEs) such as Intel Software Guard Extensions (SGX) or AMD Secure Encrypted Virtualization (SEV) to protect ML workloads running on third-party hardware [1]–[5].

A core component of neural networks are activation functions, chosen by developers (alongside other architectural decisions such as the number of layers or the learning rate) to introduce non-linearity. These functions are generally computed once for each neuron based on the sum of the multiplication of all incoming inputs by their weights (plus a bias term). Often, these functions are provided by a ML framework such as Tensorflow or PyTorch, which all include routines for training, running inference, and deploying models. It is important to note that these framework-provided activation functions usually rely on basic mathematical functions such as `std::max()` or `exp()`, often provided by the system’s standard libraries (e.g., `glibc` or `musl`) and optimised for speed, not side-channel resistance. TEEs like Intel SGX often supply their own (restricted) standard library (e.g., SGX’s `tlibc`), which provides implementations known to work within the special enclaved environment. In summary, ML frameworks inherit their security properties from the used standard library math functions.

Research into side-channel attacks (both with physical access as well as remotely exploitable side channels like timing) has led to the “hardening” of certain security sensitive algorithms, especially in cryptographic libraries.

However, less attention has been paid to the side-channel security of ML libraries, even though their parameters (weights and biases) are today often akin to cryptographic secrets in sensitivity. Especially in the context of TEE-protected ML workloads, the strengthened side-channel adversary model has not been sufficiently studied.

In this paper, we show how pervasive data-dependent memory access patterns in activation functions across many ML frameworks can lead to the deterministic recovery of hidden model parameters when deployed in a TEE. Particularly, we develop a novel methodology to recover partial weights and biases from the first (and deeper) layer(s) of a victim network when provided with an instruction-granular page-access trace. As a practical case-study attack, we deploy a Tensorflow Microlite model inside an SGX enclave and extract deterministic, instruction-granular page access traces using the SGX-Step [6] framework. We demonstrate successful recovery of each weight and bias of the network to more than 5 decimal places accuracy with 55 invocations of the network, or with less than 1% average error with around 20 invocations after an initial calibration phase. Our end-to-end attack outperforms Tramèr-style model stealing attacks [7], which require around 100 invocations for each parameter in simpler classification networks. Considering the wider ecosystem, we survey widely used ML libraries and find widespread use of secret-dependent access patterns in activation functions. Furthermore, we discuss to what extent our attack vector is applicable to other popular TEE architectures.

Contributions. Summarised, our contributions are:

- A novel methodology to recover weights and biases from partial memory-access side-channel traces.
- An end-to-end case study of practical memory-trace extraction and accurate weight/bias recovery from Tensorflow Microlite running inside an SGX enclave.
- A comprehensive survey of input-dependent accesses in common activation functions across popular ML and standard libraries.
- An open-source Tensorflow Microlite SGX benchmark for future work on attacks and mitigations.

Ethical Considerations. This work contributes to better understanding limitations of widely used TEE technology. Our attacks exploit the well-documented issue of precise monitoring of enclave memory accesses using tools like SGX-Step. All experiments were conducted on proof-of-concept implementations on our own local machines.

2. Background and Related Work

Trusted Execution Environments. One of most commonly used and widely studied TEEs is Intel’s SGX, which, even though discontinued for client CPUs, is widely supported on Xeon Scalable server CPUs and now marketed for use cases such as secure ML deployments [2]. SGX-secured code is executed in a hardware-protected ‘enclave’ (with its memory encrypted) such that even the `root` user cannot gain access. SGX does not make any guarantees about protections against timing and memory-based side channels [8], and hence is vulnerable to cache and page fault attacks [9]. SGX also allows secrets to be securely loaded into the enclave remotely,

and subsequently be (un)sealed for local storage. This allows data of the enclave (such as a pre-trained ML model) to be also protected while at rest.

Other TEEs of note include ARM’s TrustZone which brings the concept of TEE to e.g., mobile devices for isolating certain software from the user, for example, in Digital Rights Management (DRM) applications [10]. Intel’s Trust Domain Extensions (TDX) [11] and AMD’s SEV [12] are TEEs that build on application-level TEEs which provide hardware-backed isolation guarantees at the level of entire Virtual Machines (VMs). Their approach is intended to make it easier for developers to take advantage of TEE security features, because applications do not need to be ported or modified for the enclaved security model.

Though not a vulnerability per se, a consequence of SGX’s adversary model is that it allows an attacker to have precise control over the enclave’s execution. This gives rise to tools like SGX-Step [6], which allows an attacker to perfectly single-step enclaved code by causing the enclave to be interrupted, suspended, and then resumed rapidly. When paired with a more conventional side channel that can probe memory pages to detect other accesses, a precise record of a program’s execution (or trace) with respect to those pages can be recorded.

Model Stealing Attacks. The recovery of parameters of a trained neural network via “model stealing”, using the target as a opaque box, is well documented in the literature. Such practical recovery attacks have been first demonstrated by Tramèr, Zhang, Juels, *et al.*, enabling the duplication (stealing) of neural networks and other models [7]. However, they require a large number of queries, around 100 per parameter, and furthermore access to the output probabilities to essentially brute-force the space of the network. An alternative approach by Canales-Martínez, Chávez-Saab, Hambitzer, *et al.* (and references therein) treats the recovery of model parameters as cryptanalysis, showing that the *sign* information for each neuron in a 1.2M parameter CIFAR10 network can be recovered in around 30 min using a 40 GB A100 GPU [13].

Side-Channel Attacks on ML Implementations. An alternative approach to recover model parameters is to use a software-based (timing or cache) side channel. Most research in this direction has focused on the recovery of hyperparameters, such as the network’s architecture, but *not* the precise weights: Yan, Fletcher, and Torrellas demonstrate a technique for recovering the hyperparameters of a victim network such as the number of layers and their activation functions using a Flush+Reload cache attack [14]. Other works in this direction have used similar cache attacks [15], execution time [16], looked at embedded devices [17], and considered equivalent approaches on GPUs [18]–[20]. Other uses for software-based side channel attacks include the recovery of network inputs from floating point timing [21], membership inference [22], and the generation of adversarial examples [23], [24].

Because the targeted leakages are much “smaller” and hence harder to exploit, less attention has been paid to full model recovery, *i.e.*, weights and bias terms, through software-based side channels: Alder, Van Bulck, Oswald, *et al.* show how an attacker-controlled configuration of the x86 floating point unit can be used to recover weights from a toy neural network (using a custom implementation)

running in an SGX enclave [25].

Gongye, Fei, and Wahl show that, if an adversary obtains the precise timing of each network layer, in certain cases they can use timing leakages from floating point to recover the full model [26]. In particular, the authors rely on different execution timing on certain x86 CPUs when processing “subnormal” numbers. Gongye, Fei, and Wahl do not specify whether their attack applies to real-world ML libraries, and assume that the necessary precise timing measurements “can be achieved by either analyzing the cache access pattern [...] or through visual inspection of power traces”. In contrast to their work, in this paper, we consider the input-dependent memory access patterns of activation functions in widely used ML libraries, showing an end-to-end attack that uses SGX-Step for reliable side-channel observations.

In contrast, side-channel attacks that recover the full model with physical access to the hardware and measurements of electro-magnetic (EM) emanation or power consumption have been further developed [27]–[30]. However, as these attacks require measurements on or in close proximity to the targeted chips, they are of less relevance to datacenter applications, where physical access to the underlying servers is typically closely guarded.

Hence, in this paper, we focus on software-based side-channel attacks to recover weights/biases without physical access and without access to the output probabilities.

Controlled Channel Attacks. For SGX, Intel explicitly places the burden of preventing secret-dependent memory accesses for security-critical code on the developer [31]. In practice, this means that enclave developers should avoid data-dependent patterns of the form `array[x]` or `if(x) func()`, where `x` depends on a secret. It is important to note that in practice, such secret-dependent access patterns may only become evident at the machine code level, as optimising compilers might e.g., opt to compile “branchless” code into code with conditional branches, and vice versa.

Apart from well-known microarchitectural cache leakage [32], which is notoriously noisy, a number of SGX-specific side channels were discovered that exploit the privileged attacker’s control over the untrusted operating system. One of the first ones being “controlled channels” as introduced by Xu, Cui, and Peinado [33]. This method exploits the fact that page faults within an SGX enclave are handled by the untrusted operating system. A privileged adversary can, hence, temporarily unmap a page, observe whether a page fault occurs, and from this fully *deterministically* infer enclave memory access patterns at a 4 KiB, page-level spatial granularity. While such page-fault attacks have been proven particularly powerful, e.g., to extract text and images [33] or full cryptographic keys [34], their relatively coarse-grained spatial resolution may limit exploitability. Consider the example code snippet provided in Figure 1, where a tight `strlen` loop is executed that fits entirely within a single code and data page. As subsequent accesses to the same page are cached in the processor’s Translation Lookaside Buffer (TLB), and the enclave needs both the code and data page to make forward progress, page-fault adversaries only observe the first access to a page and are not able to distinguish successive `strlen` loop iterations. To overcome this limitation, Van Bulck, Weichbrodt, Kapitzka, *et al.* showed

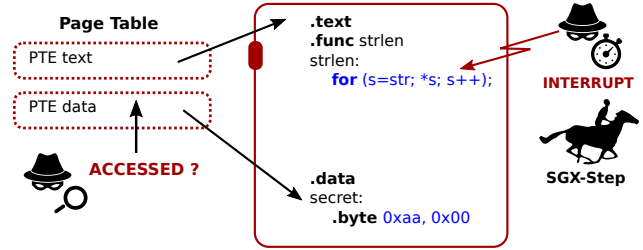


Figure 1. Victim enclaves exhibiting tight memory-access patterns can be precisely interrupted at instruction-level granularity using SGX-Step allowing to extract deterministic page-access count traces.

that privileged adversaries may also monitor page-table attributes [35] using the ‘accessed’ and ‘dirty’ bits to count accesses to a certain page.

The open-source SGX-Step framework [6], [36] allows for precise single-stepping of production enclaves using privileged x86 APIC timer interrupts, such that page access patterns can be *deterministically* monitored for every enclave instruction, giving precise insights into the operation of a victim enclave. By conservatively under-estimating the APIC timer interval, SGX-Step results in either zero or single-steps, but *always* avoids multi-steps [36, Table 5]. Subsequent works [37]–[41] showed that the accessed (A) bit in the enclave code page *deterministically* distinguishes single-steps (enclave instruction retired; A=1) from zero-steps (A=0). Intel has acknowledged perfect single stepping in a recent paper [41], which also explains the underlying mechanism to stall the CPU pipeline using microcode assists. To date, instruction-granular page-access traces extracted with SGX-Step have been repeatedly abused to reliably exploit enclave interface vulnerabilities [40] or to reconstruct cryptographic key material [38], [39]. In the following, we show that such traces are sufficient to recover weights from real-world neural network libraries running inside a production SGX enclave.

3. System and Adversary Model

We adhere to Intel’s standard SGX threat model, where the adversary has full `root` access on the victim machine, as is e.g., the case when deploying an ML model on external cloud infrastructure. Notably, we do not require physical access to the machine for our attack. Privileged software adversaries can use SGX-Step (cf. Section 2) to precisely single-step a target enclave and obtain instruction-granular page access traces. We discuss generalizations to other TEEs in Section 8

We assume the network’s weights and biases are confidential (sealed), while the enclave source code is known. The latter is a common assumption in SGX attacks [6], [32]–[35] and the default case in the Intel SGX architecture and SDK. Non-standard confidential-code deployments only add “security through obscurity” by requiring an additional, out-of-scope reversing phase [14], [42].

We assume a pre-trained ML network has been securely loaded into an SGX enclave to perform inference. We do not consider the security of the model training process, which is orthogonal to our attacks, but believe it to be

```

1 float expf(float x)
2 {
3     // ...
4     if (hx >= 0x42b17218) { /* if |x|>=88.721... */
5         if (hx>0x7f800000) return x+x; /* NaN */
6         if (hx==0x7f800000) return (xsb==0)? x:0.0;
7         if (x > o_threshold) return ...; // overflow
8         if (x < u_threshold) return ...; // underflow
9     }
10    if (hx > 0x3eb17218) {
11        if (hx < 0x3F851592) {
12            // ...
13        } else {
14            // ...
15        }
16    }
17    else if (hx < 0x31800000) { /* when |x|<2**-28 */
18        if (huge+x>one) return ...; // inexact
19    }
20    // ...
21 }

```

Listing 1. Excerpt from `expf()` in `tlbnc`.

an interesting avenue for future research. Inputs are passed into the enclave and the output is returned outside the enclave through the standard `ecall` interface. Based on the security guarantees of SGX, an ML developer would assume that their network is protected against duplication, as the inference is handled entirely within an enclave, and weights are never stored outside.

We focus on Feedforward Neural Networks (FNNs) because they effectively illustrate the problem we exploit and are easily deployable in SGX enclaves (e.g., without dynamic linking or requiring `libc`) using Tensorflow MicroLite. We also assume the network architecture (at least the number of neurons per layer and activation functions) is evident from the source code, known (as in the case of a well-known architecture or a transfer-learning model), or can be recovered via a cache attack [14].

4. Vulnerable Activation Functions

In this paper, we mostly consider activation functions that include a call or calls to a functions in the `exp()` family, e.g., `sigmoid()`, `tanh()`, and `expf()`. This is based on our initial observation that typical implementations of `exp()` contain a number of *input-dependent branches with different return cases*. To give an example, Listing 1 shows some different code paths of the implementation of `expf()` in SGX’s `tlbnc`¹. Observing the memory access/execution patterns, e.g., with SGX-Step, allows an attacker to learn which return case an input results in, and thus obtain information on the input to `exp()`. Note that while several variants of `exp()` implementations exist (both in terms of algorithms for calculation and in terms of single and double precision floats), many of them feature the same structure, where several cases are handled with different return statements.

Attacking an activation function containing a call to `exp()` is similar to attacking `exp()` directly. One must be careful to note the sign of the input (as in the case of the $-x$ in `sigmoid()`’s `exp(-x)`) and search in the correct direction. In the case of functions like `tanh()`, which include multiple discrete calls to `exp()`, the code to process the memory access traces can not assume a one-to-one relationship between a call to `exp()` and a single

TABLE 1. SURVEY OF POTENTIALLY VULNERABLE ACTIVATION FUNCTIONS.

Activation Function	Output Range	Contains <code>exp()</code>	Contains <code>max()</code>
<code>sigmoid()</code>	(0,1)	✓	✗
<code>tanh()</code>	(-1,1)	✓	✗
<code>softplus()</code>	(0,∞)	✓	✗
<code>ELU()</code>	(-α,∞)	✓	✗
<code>SELU()</code>	(-λ * α,∞)	✓	✗
<code>relu()</code>	(0,∞)	✗	✓

neuron’s activation. Another important consideration is the expressive power of the function, which we discuss in more detail in Section 5.3.

We summarise common activation functions in Table 1, and discuss their security in Section 7.2.

Despite our focus on the `exp()` family of functions, any function exhibiting measurable input-dependent variation in instruction counts (or memory access patterns) is likely vulnerable.

As long as the attacker can force a vulnerable function to process inputs that fall into multiple distinguishable classes, it is possible to search for the boundary points between these cases, as we discuss in detail in Section 5. In particular, `relu()` does not rely on a call to `exp()`, but to conditional logic or a call to `std::max()`. While `relu()` is ubiquitous, especially in ML-aided computer vision applications, transformers and other modern Large Language Models (LLMs) use a variety of `exp()`-based activation functions such as `softmax()`, `tanh()` and `GELU()` in addition to `relu()`. We discuss the vulnerability of `relu()` in Section 7.2.1.

4.1. ML Framework Functions

Thus far, our discussion of the functions used for activation functions have focused on low level mathematical used by ML framework developers inside of higher level framework code. A Tensorflow neuron with `tanh()` activation might not, for instance, directly return the output of a call to math library’s implementation of `tanh()`; there might be wrapping or processing of the result. This is of interest as we can also exploit input-dependent behavior at this higher framework or application level.

An example of this is the code to Tensorflow lite’s `sigmoid()` function (called `Logistic()` in the source), shown in Listing 7 in Appendix B. We can see that on top of any side-channel leaks due to calls to `std::exp()`, a higher-level set of memory access patterns and instruction count cases are introduced by a conditional routing to different functions (or simply a return of 1) based on the input. In this way, this `sigmoid()` function can actually be attacked at two levels which we will describe in Section 6.2.

5. Methodology

First, we describe the overall concept for our attack (Section 5.1) against a neural network. We then explain in more detail how to attack the first layer (Section 5.2) and finally the subsequent layers (Section 5.3).

1. https://github.com/intel/linux-sgx/blob/7385e1/sdk/tlibc/math/e_expf.c

5.1. Attack Concept

The starting point for our attack is the above observation (cf. Section 4) that, unlike in cryptographic libraries, the math functions that underpin many ML activation functions have not been hardened to ensure they execute in constant time and without input-dependent branches and memory access patterns². We believe this work has not been undertaken in the context of ML due to performance concerns or because security is seen as less of a focus.

By examining the underlying functions statically, dynamically, or by reading the code (if available), we can deduce the possible branches through the function and the timing as well as memory access patterns therein. Also of interest are cases where certain input values are handled differently (via multiple `return` statements). A special case of those are *early returns*, where certain inputs cause the function to return before the full output is computed.

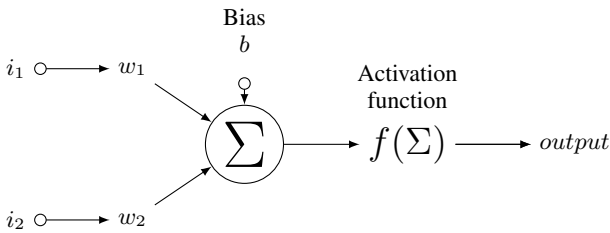


Figure 2. Visualization of a single 2-input neuron. We use Σ in this paper to represent the sum of all $i_i * w_i$ and b passed into an activation function.

Given that such code patterns take different numbers of instructions (and exhibit different memory access patterns) depending on the input, we can more generally assert that there is a correlation between different code paths and the execution trace. Though these differences might be subtle (e.g., a single instruction), they are measurable given a suitable side channel. Thus, if an attacker can determine which branch a function has taken, they learn something about the input or argument to that function.

As mentioned before, one function with these properties is `expf()`. Figure 3 shows the 11 different return cases of this function based on input and their associated CPU instruction counts (collected using `gdb`). We note that we found other optimised implementations of `expf()` that all use a similar algorithm and thus exhibit the same input-dependent memory access patterns. We focus here on the one used by SGX `tlIBC`. For ease of discussion we labeled these cases using the names shown. For example, `expf(4)` puts us in case Normal (+), whereas `expf(110)` results in the Overflow case. We define a *threshold* (shown in Figure 3 as dotted black lines) as an input value that is on the precise border of two output classes. For example, 88.72168 is the value between Normal (+) and Overflow.

We can also use knowledge of these regions and thresholds in the other direction: for example, if we know that an execution of `expf()` takes 17 CPU instructions (placing us somewhere in the Overflow region), we

know the input to that function call must be greater than 88.72168. We note that the cases for Overflow and Underflow are both early returns and as such their instruction counts are much lower than the other ‘normal’ returns which actually perform some sort of unique computation.

We can use these threshold values to leak information about the precise value of a partially controlled input. If we consider the scenario where an input to `expf()` is being multiplied by a hidden constant c and we have access to the instruction count of the execution, we can reveal c by finding (via e.g., a binary search) a threshold value between two instruction count classes and then dividing that value by our input. For example, if we find that the input 3.2164 multiplied by c leads to threshold value 88.72168, c must be $88.72168/3.2164 \approx 27.5842$. We therefore define 3.2164 as a *convergence point*: an input to the system that causes a threshold value and thus a leak of the precise input to the function.

We now extend the above into a chosen input attack against a toy ML network. Consider an attack against a simple neural network with only a single neuron, as shown in Figure 2. The activation function is simply `expf()`. The goal is to recover w_1 , w_2 , and b . We are free to choose values for i_1 and i_2 . We first note that the input to a neuron’s activation function is the sum of the products of various user-controlled inputs and their hidden weights, plus a hidden bias term (Σ in Figure 2); this is similar to the case described previously except we have two hidden constants multiplied by two different inputs and an additional term, the bias, that is never multiplied with our inputs.

If there was no bias term, we could simply use a variant of the approach described above and iterate through each input (setting all other inputs to zero, allowing us to focus on one weight at a time) and recovering each parameter independently. The addition of the bias term adds another unknown which means we can only find through constraints on the value of the hidden weights and bias:

$$\begin{aligned} i_1 * w_1 + 0 * w_2 + b &= 88.72168 \\ \Rightarrow w_1 &= \frac{88.72168 - b}{i_1} \end{aligned}$$

To solve for all three unknowns, we find enough sets of values (one for each input to the neuron) to generate a system of equations to solve for as many unknowns as we have (number of weights plus bias term), for example:

$$\begin{aligned} i_1 * w_1 + 0 * w_2 + b &= threshold_1 \\ 0 * w_1 + i_2 * w_2 + b &= threshold_2 \\ i_3 * w_1 + i_4 * w_2 + b &= threshold_3 \end{aligned}$$

Here, we define $(i_1, 0)$, $(0, i_2)$, and (i_3, i_4) as *convergence point sets*, because each set of chosen inputs forces the activation function to a threshold value. Once we have enough equations (one for each unknown), we solve using linear algebra for the unknown weights and biases. Note that the thresholds do not have to be different, though the more thresholds are hit, the more robust the solution.

2. A classic example in the cache timing literature is Look-Up Tables (LUTs) that may be accessed in deterministic patterns based on the function inputs.

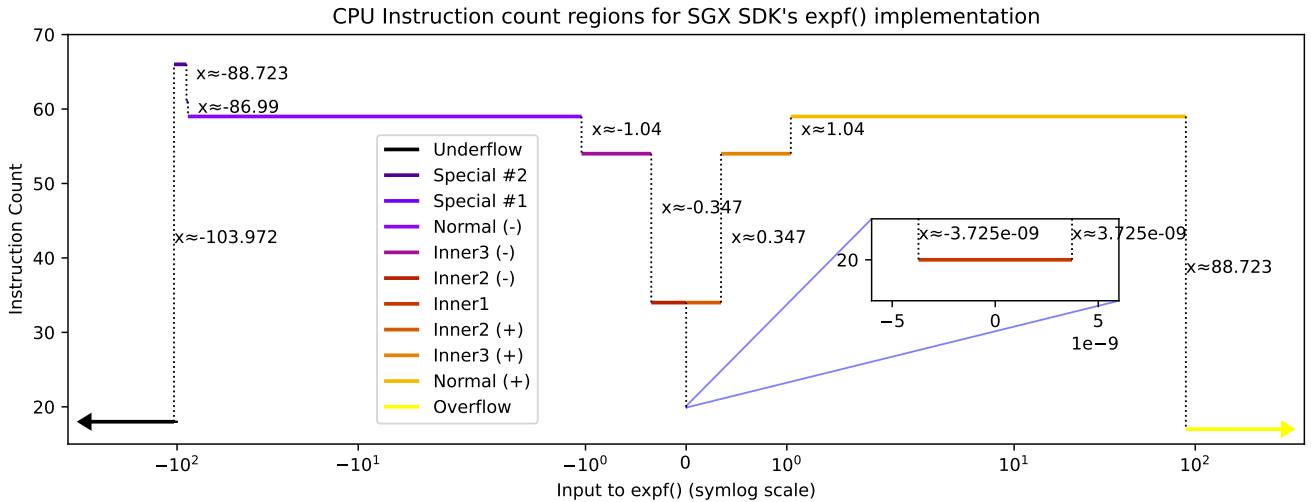


Figure 3. Visualization of $\exp f()$ CPU instruction count regions by input. The Underflow and Overflow regions have different instruction counts: 18 and 17 respectively. Note also the symmetrical regions of Inner1, inner2, and Inner3.

Though it is possible to find convergence point sets like $(i_1, 0)$ and $(0, i_2)$ above where all but one input is locked to zero and the remaining input is used to search for a threshold point, this is not required. In fact, by locking all but one input to some small magnitude random numbers (for example, i_3 in the third equation) and searching on the single unlocked parameter (i_4), an arbitrary number of convergence point sets can be found.

Finally, if we replace $\exp()$ above with a different function (such as $\text{sigmoid}()$) that also leaks threshold values, the only thing that changes is how to conduct the binary search: the recovery procedure is otherwise identical. Building on this concept, we will show how it is possible to recover the hidden parameters of more complex networks to a high degree of accuracy.

5.2. Full Attack on First Layer

Continuing on from Section 5.1, we discuss how to attack the first layer of a production neural network. As before, the goal of this phase is to find a number of convergence point sets equal to the number of inputs plus one in order to have a system of equations we can solve to recover the weights and bias.

The first layer may be a special case if (without loss of generality) there is no filtering or normalization which pre-processes the input values. If this is the case, we can choose any values we want to feed into the network (we can not immediately inject values deeper into the network). If there is filtering or normalization, however, we treat the first layer like all subsequent layers.

If we can inject arbitrary values into the first layer, we iterate over every neuron in the first layer and recovery its hidden parameters in 2 phases: calibration and binary search.

5.2.1. The Calibration Phase

In the first phase, we quickly produce sensible starting points and context for the second phase of the attack. We prepare a test input to the network that is all small non-zero values but set the first value of the array to a large

value. If we run this test input and detect that the neuron overflowed, we know that this input is large enough to cause an overflow and that the weight between the first input and this neuron must be positive. If instead we produce an underflow, we know that the weight must be negative. If we are not in an overflow or underflow state (perhaps owing to a low magnitude weight). In this case, we simply multiply the large value in our test input by 10 and try again. We continue in this way until we find the sign and magnitude required to over/underflow this neuron from each input to the network. Note that we do not actually binary-search towards a threshold between two cases here; we merely attempt to reach an overflow/underflow case. In this case, we do not need to find a threshold for the instruction count leak to be informative.

Recovering the signs for each weight is useful since some of the cases (most of the “normal” ones) are symmetrical about zero, meaning we cannot learn the sign of the input only based on the state. Recovering the sign before we begin the binary search means we always know exactly where we are in the state space. Recovering a value that overflows/underflows the neuron is useful to accelerate the attack. Though we could choose the maximum float value for the starting point of our binary search, the lower the initial guess, the fewer steps the search has to take. Searching “up” in the calibration step and then searching down in the second phase reduces the number of invocations needed.

5.2.2. The Binary Search Phase

Armed with the information collected in the calibration phase, we continue the attack against the same neuron in phase 1. Now, we can binary search to find the desired number of convergence point sets for this neuron. For as many convergence sets as we need, we start by generating an input set that is made of n locked random values (one for each input) except that the i 'th input is instead set to the large positive value recovered during calibration. We feed the input into the network and note the return case by interpreting the CPU instruction counts for each neuron. Even if some of the weights have different signs,

the overall Σ should be dominated by the large input multiplied by its weight. If the neuron has overflowed, our input has caused the neuron to enter the state above the threshold between normal (+) and overflow and should search down. If the neuron has instead underflowed, we must be in the boundary between underflow and normal (-). If the input is negated before entering `exp()` as in `sigmoid()`, the direction to search should be reversed. We continue the binary search on that i 'th input (searching back up if we fall below an underflow/overflow case in terms of magnitude) until we hit the desired search depth or our search does not change, because we reached the limit of decimal places for a floating point number. The tradeoff between depth and speed is shown in Table 2.

Using this algorithm, we can generate as many novel convergence sets as we require since the unchanging members of the input set are all randomised between inputs. It is worth noting that the system of equations does not produce usable results if the values on the right hand side are all the same threshold, so targeting multiple thresholds is required. One quick way to find more thresholds for the system of equations is to flip the signs of the inputs to ensure both the underflow-to-normal and overflow-to-normal thresholds are included in the solution set. Note however that it is not required to target the thresholds between underflow/normal and normal/overflow; these are just the easiest to find since we can force an under/overflow and then work our way up/down until we find the normal region. There are other thresholds within `exp()` (as shown in Figure 3) that can be exploited if they can be reached so long as we know the sign of the weight and thus in which precise state we are in.

Once we have the requisite number of equations, we can solve the system of equations as described in Section 5.1 to recover the weights/biases for this first neuron. We then perform the exact same two-part algorithm on each remaining neuron until we solve the entire layer. The output from our recovery tool as it recovers one neuron is depicted in Appendix A.

5.3. Extending the Attack to Deeper Layers

In order to extend the attack into subsequent layers, we must solve two key problems. First, how can we ‘unwrap’ the effect of already-solved early layers to insert arbitrary inputs beyond them, deeper into the network? And second, is it always possible to generate those values?

Unwrapping Solved Layers. Our attack methodology for the first layer relies on being able to precisely craft a set of “target” in order to search towards threshold points. In order to be able to do this for deeper layers, we first have to “unwrap” all the recovered layers between the input layer and the layer we target. In the following set of equations, we show how to rearrange the normal operation of a neuron to isolate the input as opposed to the target.

$$\begin{aligned} \text{act}(\text{input} * W + b) &= \text{target} \\ \text{input} * W + b &= \text{act}^{-1}(\text{target}) \\ \text{input} * W &= \text{act}^{-1}(\text{target}) - b \\ \text{input} * \cancel{W} * W^{-1} &= (\text{act}^{-1}(\text{target}) - b) * W^{-1} \\ \text{input} &= (\text{act}^{-1}(\text{target}) - b) * W^{-1} \end{aligned}$$

Note that it is also possible to do this without matrix inversion for greater numerical efficiency, e.g., using `numpy.linalg.lstsq(W, act_inv(target)-b)`.

In these equations, *act* and *actinv* are known since we know the architecture of the network and W and b are known because we already solved this layer. Therefore, given a solved layer’s hidden parameters, a desired ‘target’ set of values, and the appropriate inverse activation function, we can calculate the input we must feed into the layer to produce a desired target as the output of that layer. Note also that the above assumes the activation function is invertible without a substantial loss of accuracy. Inverting these functions might lead to an inability to pass certain values forward, which we discuss below.

Expressive Power. Even if we can algebraically calculate how to pass arbitrary values through a solved layer, subsequent layers are harder to attack because we are limited by the “expressive power” (see Table 1) of the neurons before the target layer in terms of both magnitude and sign. There are two consequences to this.

The first is some values may be impossible to generate in subsequent layers. For example, since the output of `sigmoid()` is always positive, barring negative biases, it would be impossible to send negative values into the next layer. Similarly, `relu()` can never produce a negative output. The second is that certain thresholds such as those between `expf()`’s overflow/underflow and normal cases have a high magnitude ($\approx 88.723-103.972$) relative to generally smaller magnitude weights and biases. `sigmoid()` has a very small output range (0–1) making it impossible to produce a large enough Σ in the next layer to ‘reach’ one of these two thresholds unless either the network is very dense with small-magnitude positively weighted neurons or has some positive and large magnitude (> 1) weights connected to it. This suggests denser networks are more expressive and therefore more vulnerable. In both of these cases, we rely on certain key hidden parameters, which means that certain networks might not be vulnerable to our attack. We however note that security guarantees should never assume a certain network architecture.

Attack Outline. Nevertheless, extending the attack into deeper layers is possible with certain caveats. There is no need to focus only on the high magnitude thresholds we previously discussed between the underflow/overflow cases and the normal one; there are six in the range from $\approx -1.04-1.04$ (see Figure 3). By searching anywhere within this region (e.g., near the subnormal case as in [26]) we can, as before, build convergence sets for our inputs and solve for the hidden parameters. Because we might pass through a low expressiveness activation function like sigmoid (output range from 0–1), which is likely

being further reduced by multiplication with a weight with magnitude <1 , we might not cross a single threshold point (the presence of the bias as a component of Σ means that we might be shifted away from zero far enough that we cannot reach both sides of the subnormal case).

As such, we instead start with a grid search to scan (at some resolution up to the attacker which trades off speed and the chances of finding a narrow instruction count class) for multiple instruction count classes. As with the binary search, we start by creating an input set that is made up of n locked random values (one for each input) except that the (randomly chosen) i 'th input is nominated as a dynamic value, initially set to a high magnitude positive number. We scan the dynamic value from its initial value down to a high magnitude negative number, we can check to see if encounter multiple return cases. If we are able to reach multiple classes, we can then perform a binary search between those classes to isolate the threshold and build a convergence point set, as before.

6. Implementation and Orchestration

We trained several neural networks using “full” Tensorflow (in Python). In this section, we will first introduce a proof-of-concept attack on a case-study victim network with an `expf()` activation function. Next, we show how to attack a more realistic activation function and start to recover partial information from deeper layers.

6.1. Regression Model with `expf()`

Model. We first focus on a regression model to predict home insurance costs, which was trained on the “Medical Cost Personal Dataset” [43]. The network has three hidden layers. The first hidden layer contains 100 neurons that use the `Exponential()` activation function which is just a direct call to `expf()`. There are 11 input nodes, meaning that there are in total 1200 parameters (1100 weights and 100 biases) that we target. After the first layer, there is a second hidden layer of 10 neurons which uses a `relu()` based activation function. A final layer contains a single `relu()` neuron.

For this first network, we only focus on the first hidden layer. Despite that, we note that:

- 1) These choices give us the clearest method to discuss and explain the underlying vulnerability (secret-dependent control flow).
- 2) More complex networks or types of networks do not inherently offer greater security unless the underlying problem is addressed, even if demonstrating the attack might be more technically challenging.
- 3) The attack is agnostic to the accuracy of the network.

Victim Enclave. The enclave code runs inside of SGX. Given the constraints of SGX’s standard library replacement `tlibc`, we decided to employ Tensorflow Microlite, a software package for running (converted) Tensorflow lite models on microcontrollers, instead of “full” Tensorflow (which relies on a variety of system calls not easily provided by SGX). Our SGX enclave thus included a statically compiled Tensorflow Microlite library to perform inference. We converted our tensorflow models to `tflite` and then further exported them as to a byte

array which can be compiled directly into a C program. These byte arrays are added to the enclave code which allows us to perform “secure” inference inside SGX. We note that for practical deployments of SGX-protected ML, using such a reduced variant of Tensorflow would ease deployment, reducing code and thus Trusted Computing Base (TCB) size, while maintaining compatibility with Tensorflow-trained models. The underlying implementation [44] of `exp()` used by our network during inference comes from SGX’s `libc` alternative, `tlibc`.

Attack Code. To practically execute our attack, we used SGX-Step to collect the CPU instruction counts necessary to understand the state of our victim networks and apply the steps described above. Using SGX-Step, we developed an attack application, which starts the enclave and interacts with it. We use this to record page accesses which we later interpret into activation function states. Using SGX-Step, we log all page accesses within the enclave (after a certain trigger page was accessed) and interpret the results as part of a post-processing step.

Post-Processing. Once Tensorflow Microlite ran within an enclave, we profiled the execution and observed call traces (via `sgx-gdb`) to understand execution flow. An example can be seen in Listing 2. This lets us build an intuition for how Tensorflow Microlite performed inference and which functions and pages are accessed.

```

1 0x7ffff762b460 in expf()
2 0x7ffff7625e9c in tflite::(anonymous namespace)::
  ExpEval()
3 0x7ffff762318b in tflite::MicroInterpreterGraph::
  InvokeSubgraph()
4 0x7ffff760f04e in performInference()
5 0x7ffff7610577 in entry_point()
6 0x7ffff7611633 in sgx_entry_point()
7 0x7ffff76130a2 in do_ecall()
8 0x7ffff762c5a5 in enter_enclave()
9 0x7ffff762c7d5 in enclave_entry()
10 0x7ffff7f95309 in __morestack()
11 0x7ffff7f986fb in CEnclave::ecall()
12 0x7ffff7f9a852 in _sgx_ecall()
13 0x55555555bac9 in entry_point()
14 0x555555557a24 in main()

```

Listing 2. Simplified call stack for `expf()`-based neuron in Tensorflow Microlite.

Unlike `sgx-gdb`, SGX-Step only offers a relatively coarse-grained spatial resolution of 4 KiB memory pages, which prevents production enclave attackers from directly identifying the specific symbol (e.g., function or data) accessed by the enclave code. However, SGX-Step’s precise instruction-level temporal resolution enables the annotation of coarse-grained page-access traces with the exact number of instructions executed on each page. As illustrated in Figure 4, this capability allows to accurately reconstruct the inference execution structure, even without knowledge of the lower 12-bit page offset of the secret enclave instruction pointer (ERIP). By comparing the dotted red line which depicts the true ERIP values available to `sgx-gdb` and the black line which shows the reduced page-level granularity, one can see how little is lost. It is worth nothing that each page can contain multiple functions and so it is difficult to assign a precise “meaning” to each page without context. The instructions executed on one page could pertain to two very different activities at different points in execution. However, the combination of coarse-grained page-access patterns along with the exact

amount of instructions executed per page, annotated in black text, clearly suffices to identify individual function calls or data accesses. In practice, this means that even if multiple symbols are co-located on the same 4 KiB page, we can still interpret the logs. We also know precisely the length (or length range) of different runs at different points during the execution, *i.e.*, we can also tell if a trace is invalid and immediately reject it.

By studying inference traces from the perspective of both `sgx-gdb` and `SGX-Step` (raw traces or visualizations like those shown in Figure 4), clear patterns emerge. For example, the function `ExpEval()` is located on a different page to `expf()` (each `0x1000` bytes is a new page) and we can plainly interpret the movement between them as the higher level neuron code invoking the lower level `expf()` math function 16 times (once for each neuron in this layer). The 18 instruction count long runs at the extreme left and right on page `0x2c000` seem to correspond to the start and end of a layer, which makes parsing each layer trivial. We note that the step counts provided by `sgx-gdb` and `SGX-Step` may vary slightly (but deterministically) due to the documented effects of macro-op fusion [38].

The final part of our tooling is a Python script and library which further abstracts and manages invocations of the enclave program. Because each neuron is accessed in order and each return occurs in sequence, it should be possible to monitor each neuron’s step count independently. In order to orchestrate the full attack, we use this script to interpret the log output by `SGX-Step` into a per-neuron state. Even though we receive the state for every neuron in each log, we only focus on one at a time. An example output of the running attack is shown in Listing 6 in Appendix A.

6.2. Multi-Layer Model with `sigmoid()`

Model. We now focus on a “multiplication” network (trained to multiply numbers), a small network with the following architecture: there are two inputs, followed by the first hidden layer which contains 4 sigmoid neurons. Then there is a second hidden layer containing 8 sigmoid neurons followed finally by the final layer with a single `relu` neuron.

Recovery. We follow the steps described in Section 5.2 and Section 6.1 to recover the first layer using the exact same attack code. The only difference is that we exploit a different CPU instruction count leakage; instead of targeting `tlibc`’s exponential function, we now attack the Tensorflow lite framework-level sigmoid function as described in Section 4.1. This shows how our attack is adaptable to different and more realistic activation functions, as well as side channel leakages elsewhere in the ML inference pipeline, cf. Section 7.1.1.

7. Results

We integrated our victim enclave, performing inference using our Tensorflow Microlite network, with `SGX-Step` for side-channel observations and our attack script for weight and bias recovery.

In Section 7.1 we discuss the results from the attack against the proof of concept regression network. In

Section 7.2 we discuss how our findings relate to other activation functions in other ML Frameworks. As a part of that, we more explicitly consider `relu()` (Section 7.2.1) and framework code itself (Section 7.2.2).

7.1. End-to-End Attack Case Study for Tensorflow Microlite Enclave

Our attack was able to fully recover all the weights and biases for the neurons in the first layer of a Tensorflow Microlite network running inside an SGX enclave. After calibration, the full attack took 55 binary searches of the network per parameter to recover each of the 1200 parameter in the first layer down to or beyond 3 decimal places of accuracy.

During the attack, each first-layer neurons’ parameters were recovered at around 99% accuracy (when compared to the ground truth values) by <36% of the way through the full search (around search depth 20). The average error is <1% at this point. The error continues to slowly improve until the search hits the limits of a 32-bit floating point number at around depth 55. These findings are further summarised in Table 2, which shows how the achieved average and maximum error in the recovered weights and biases varies with the number of queries per neuron in our 11 input regression ‘victim’.

The maximum error rates were higher in our full attack on the regression network than we had seen in smaller scale testing. We speculate this is due to numerical precision issues when solving certain neurons, particularly ones with very small weights or perhaps a combination of very low and very high magnitude weights. During the binary search there may be an ideal magnitude for the non-dynamic input values based on the magnitude of the dynamic input. We consider this an area for future study and discuss a workaround below.

The speed (e.g., number of invocations) is dependent on the architecture of the network (the number of parameters to recover) but also some factors the attacker can control such as the depth of the binary search. For example, the attack can be sped-up by only binary searching to a certain depth of iterations. As can be seen in Table 2, we already achieve an < 1% average error rate by depth 20. Based on the desired level of accuracy, an attacker can choose to only search to some depth, rather than letting the binary search finish. We note that achieving sub 1% precision may not be as necessary as it seems. As the widespread adoption of quantization has shown, some models are still accurate with the precision loss due to the conversion to 8 bit integers.

In general, the total number Q of queries to recover the first layer can be computed as:

$$Q = P \cdot N \cdot S$$

where P is the number of hidden parameters (in the first layer, e.g., one weight per input plus one for the bias) to solve for, N is the number of neurons in the first layer, and S is the maximum number of steps in the binary search.

The P value correlates to the minimum number of equations we require to solve a system of equations: one for each unknown. We can compensate for noise

TABLE 3. AVERAGE AND MAXIMUM ERROR FOR DIFFERENT SEARCH ITERATIONS OF 2-INPUT MULTIPLICATION NETWORK.

Iterations	Average error	Max. error
5	5.104921006404077	17.916865999472293
10	1.6756457515509167	17.51883507815715
15	1.5295341684026322	17.520958313634686
20	0.06962602190494313	0.7988771642785077
25	0.002053382484092837	0.023557097950552608
30	4.133456316032444e-05	0.0004519024401035132
35	3.313471981702896e-05	0.00036192843021964904
40	3.2159960239434036e-05	0.0003506233064154429
45	3.215762491123297e-05	0.00035059400594272816
50	3.215754896549253e-05	0.0003505930825000725
55	3.21575691725288e-05	0.0003505933114027471

a duplicate results in the recovery of hidden parameters that are accurate but not necessarily precise to the original source network. While they may be reconstruct the overall structure and general features of the network correctly, it remains an open question how effective they are at reproducing the specifics of the original network, as in the case of being able to craft adversarial examples from a duplicate network that still work on the original. In contrast, a more complex version of our attack that can recover all the hidden parameters with high precision could be useful in context where fidelity to the original network is desirable. However, as summarised in Table 2, our attack can also be executed with an emphasis on speed over precision, with complexity below the attack of [7]. We note that the attack in the original paper only targets classification networks and not continuous output networks like the ones in our case study.

7.1.1. Results for Multiplication network

This recovery is summarised in Table 3 and is comparable to the results of our attack against the other model.

We are also able to recover partial (signless) convergence sets for the neurons in the second layer. For example, we can recover 35 sets for the first neuron in the second layer. Given its 4 inputs and single bias term (5 total unknowns) these are many more convergence point sets than we would need for a solution. However, because we do not have sign information, we are unable to conclusively solve for the neurons’ parameters.

7.2. Activation Function Safety Ecosystem Study

In order to extend our findings and consider the breadth of the issue, we examined implementations of common activation functions to determine in popular ML frameworks to assess if they exhibit input-dependent memory access patterns. For this, we used a combination of static (Ghidra) and dynamic (gdb) analysis to explore the often complex call stacks of these frameworks until an underlying math function was reached. Our findings are summarised in Table 4.

There are several dimensions to our survey: first, we found that in all cases we tested, the low-level math functions that underpin activation functions are not included in the ML frameworks themselves. Instead, they rely either on additional high performance math libraries, e.g., `sleef` in the case of PyTorch, Eigen and DNNL in

the case of Tensorflow and XNN in the case of Tensorflow Lite or call into standard libraries like `tlibc` (in the case of SGX) or `glibc` on a Linux system. In some cases, these frameworks do both for different functions, adding to the complexity of the analysis.

The (in)security of an activation function can stem from the underlying library and implementation of these functions. For example, a call to `sigmoid()` that ends up in `glibc`’s highly input-dependent `exp()` in `libm.so` exposes the caller’s ML framework to vulnerability. Similarly, a call to the same function in a different framework that ends up in a highly optimised math library like Eigen may be harder to exploit. However, as we note in Section 4.1 and Section 6.2, higher level framework code can also be the culprit of exploitable memory access patterns. The hardware context may also play a roll in vulnerability; an Internet of Things (IoT) device performing inference on an embedded system for example may not have the hardware functionality or enough space for advanced math routines beyond a basic standard library.

The reason optimised math libraries may be harder to attack is that their use of vectorised instructions (for example AVX on Intel or NEON on ARM) which discourage branching (since that can affect performance). For example, we observed that in PyTorch, `softmax()` was realised through calls into the `sleef` library, which at default optimisations compiled into AVX assembly code without memory access leakage. We note however that `sleef` incorporates a `dispatch` mechanism that calls into different implementations depending on the outcome of `cpuid`. Notably, if this library was used in an SGX enclave, where `cpuid` is typically implemented as an `untrusted` `ocall`³, the adversary could spoof the `cpuid` result and force usage of the insecure non-AVX version. Curiously, for `sigmoid()`, PyTorch resorts to the standard library implementation of `exp()`, rendering the implementation insecure independent of `cpuid`. Tensorflow uses Eigen for all the functions we tested except for `Exponential()`, which calls directly into `glibc`. Finally it is worth restating that even though vectorised code is non-branching, it still may not be constant time, which we discuss further in Section 8.3.

Finally, Table 4 shows how the optimisation level has a direct impact on the security of `relu()` in the case of Tensorflow Microlite as further discussed in Section 7.2.1. While the compiler default of `-Os` happens to be free of memory access leakage, this is more by accident than by design, which is not desirable in the case of libraries that handle sensitive data. Analogously, the security benefits (with regard to the attack we have demonstrated) of vectorised code is not a proactive security-related decision but a side effect of pursuing performance.

7.2.1. Vulnerability of `relu()`

In addition to `expf()`, we also considered `relu()` and its implementation in Tensorflow Microlite, which relies on the `std::max()` function. When running inside of an enclave, the `std::max()` library call is provided by an implementation in SGXs `tlibc` library which can be seen in Listing 3). With the default settings (`-Os` passed to the compiler, `gcc 11.4.0`, and

3. https://github.com/intel/linux-sgx/blob/80a662/common/inc/sgx_tstdc.c

TABLE 4. SURVEY OF VULNERABILITY ACROSS VARIOUS ML AND STANDARD LIBRARIES AND FOR DIFFERENT OPTIMISATION LEVELS.

ML Framework	RELU	Exponential	Sigmoid	Softmax
TFLiteMicro (SGX/tlibc, -O0)	X	X	X	X
TFLiteMicro (SGX/tlibc, -Os)	✓	X	X	X
TFLiteMicro (glibc, -Os)	✓	X	X	X
TFLite (glibc)	✓	X	✓	✓
TensorFlow CPU (glibc)	✓	✓	✓	✓
PyTorch (glibc)	✓	n.a.	X	✓*

Legend: ✓: Secure X: Insecure due to data-dependent access pattern
*: Only secure if cpuid indicates AVX support

```

1 template <class _Tl>
2 struct __less<_Tl, _Tl>
3 {
4     _LIBCPP_INLINE_VISIBILITY
5     _LIBCPP_CONSTEXPR_AFTER_CXX11
6     bool operator() (const _Tl& __x, const _Tl& __y)
7     const {return __x < __y;}
8 };
9
10 template <class _Tp, class _Compare>
11 inline _LIBCPP_INLINE_VISIBILITY
12 _LIBCPP_CONSTEXPR_AFTER_CXX11
13 const _Tp&
14 max(const _Tp& __a, const _Tp& __b, _Compare __comp)
15 {
16     return __comp(__a, __b) ? __b : __a;
17 }

```

Listing 3. std::max() source code from sgxsdk/include/libcxx/algorithm.

the function marked as inline), the above code was compiled into branchless (e.g., UCOMISS) instructions as shown in Listing 4. In contrast, when compiling with -O0, the function was assembled with conditional branches as shown in Listing 5. This is significant because when the compiler emitted jmp-class instructions, it was possible (using sgx-gdb) to detect the single step difference and therefore discern between the cases where $input \leq 0$ and $input > 0$. This is a threshold point between two instruction count classes about 0.0, similar to the ones discussed previously in `expf()`. Though the difference might only be a single CPU instruction (whether a jump was taken or not) this difference is detectable.

Within the our case study, `relu()` within Tensorflow Microlite was not vulnerable, but it was not secure by

```

1 00100a04 MOVSS  XMM0,dword ptr [param_2]
2 00100a08 UCOMISS XMM0,dword ptr [param_1]
3 00100a0b MOV    RAX,param_1
4 00100a0e CMOVA  RAX,param_2
5 00100a12 RET

```

Listing 4. Resulting assembly for `std::max()` at -Os with gcc 11.4.0.

```

1 001019c9 PUSH  RBP
2 001019ca MOV   RBP,RSP
3 001019cd MOV   qword ptr [RBP + local_10],param_1
4 001019d1 MOV   qword ptr [RBP + local_18],param_2
5 001019d5 MOV   RAX,qword ptr [RBP + local_10]
6 001019d9 MOVSS XMM1,dword ptr [RAX]
7 001019dd MOV   RAX,qword ptr [RBP + local_18]
8 001019e1 MOVSS XMM0,dword ptr [RAX]
9 001019e5 COMISS XMM0,XMM1
10 001019e8 JBE   001019f0
11 001019ea MOV   RAX,qword ptr [RBP + local_18]
12 001019ee JMP   001019f4
13 001019f0 MOV   RAX,qword ptr [RBP + local_10]
14 001019f4 POP   RBP
15 001019f5 RET

```

Listing 5. Resulting assembly for `std::max()` at -O0 with gcc 11.4.0.

design either. This is worrisome because in contrast to vetted cryptographic code, ML libraries currently **do not** exhibit input-independent memory access and execution behavior, and further the eventual security properties of high-level ML code may depend on compiler optimizations and other non-explicit behavior as with `relu()` in some configurations. Without any specific safeguards taken, ML libraries are not intrinsically secured against the vulnerability discussed in this paper.

As a sidenote, though not considered in this paper, we note that on x86, many floating point instructions can raise exceptions or otherwise exhibit operand-dependent timing as mentioned by [26] and (in a different context) [45], which might result in timing vulnerabilities even if branchless code is emitted. We leave the exact measurement and exploitation of such timing side channels in real-world settings as an area for future research.

7.2.2. Vulnerability of Framework Code

As discussed in Section 4.1, and demonstrated practically in Section 5.3, exploitable memory access pattern vulnerabilities can exist outside mathematical library code in ML frameworks themselves. This further supports our case that these frameworks are not suitable for enclave execution under a Side-Channel Analysis (SCA) advisory. Beyond the security properties of the libraries they use, security-conscious ML framework developers need to also consider their own code and if they are introducing exploitable timing side channels. This is especially true for more complex activation functions like `softmax()` which are not common mathematical functions likely to be found in standard math libraries.

8. Discussion and Mitigations

First, we demonstrated that SGX-protected ML implementations can exhibit vulnerabilities due to oversights in their implementation, leading to extraction of precise model weights and biases. Our proof-of-concept shows that an attacker with a high-resolution controlled or side channel is able to exploit data-dependent memory accesses to recover model details, whereas prior software side channel attacks typically only recovered hyperparameters such as model architecture [14]. Though there are certain limitations, precise weight recovery can be performed with at maximum 55 queries per weight, and at over 99% accuracy at less than half that number (plus calibration). Speed can be parametrically adjusted to account for the desired accuracy.

While our attack demonstration focused on the popular Intel SGX architecture, the underlying insights and weight-recovery techniques are applicable to other TEEs. Notably, the required side-channel primitives offered by SGX-Step, *i.e.*, precise single-stepping and page accesses, have been demonstrated on alternative VM-based TEEs like AMD SEV [46] and Intel TDX [47], [48].

Ultimately, while not in the scope of this paper, we believe that if an attacker can obtain precise-enough timing measurements, similar attacks may be possible outside of a TEE context, e.g., for virtualised cloud deployments. Cache attacks with high temporal resolution, e.g., Prime+Scope [49], could be applicable to recover the

access patterns similar to SGX-Step, though attacks would likely require modifications to deal with increased noise.

We further show that input-dependent memory accesses and branching are prevalent in ML implementations, and that the necessity for secure programming practices is not widely understood in the ML community.

Even if the attack described in this paper currently does not apply to non-enclaved targets, we argue that ML library developers should pay attention to the implementation attack surface. For example, even if `relu()` implementations were often secure in the surveyed libraries, this largely relied on certain compiler optimizations and was not ‘by design’. Similar to cryptographic libraries, ML libraries should hence consider hardening their codebase against software side channels such as data-dependent memory access patterns.

Security and privacy-sensitive algorithms, to which ML now belongs, must be robust by design, regardless of context, platform, or (mis)use of library interfaces by a programmer.

8.1. Countermeasures

As with the work done in cryptography libraries, there are established steps to avoid data-dependent branching and memory accesses, for example by relying on bitwise logical operations, constant-time conditional moves, and other related techniques. For x86, as discussed for the `sleef` library, using vectorised SIMD code can also mitigate the issue, though needs to be thoroughly vetted for other side channels like floating point timing [26], [45].

At present, akin to a “chosen plaintext” attack for cryptographic algorithms, our attacks entails sending arbitrarily large or small floating point numbers into the network. Any input normalization or quantisation might mitigate the fast calibration and binary search approaches described in this paper, only enabling partial recovery through the grid search technique. Similarly, as the attack requires a large number of queries to the network, rate-limiting or detection of “suspicious” usage would render exploitation harder in practice. However, again, ML security should in our view not rest on developers having to normalise inputs or limit performance, so these measures are supplementary to a securely developed library.

Finally, researchers have explored defenses at the level of the TEE itself to not fully eliminate side-channel leakage, but frustrate exploitation in practice. Initial approaches [50]–[52] focused on detecting suspicious interrupt rates as a side-effect of an ongoing controlled-channel attack, which may be error-prone and suffer from false positives. Alternatively, custom oblivious RAM solutions [53]–[55] may probabilistically hide secret-dependent enclave memory accesses, however this is at the cost of prohibitive performance overheads. Most prominently, AEX-Notify [41] is a recent Intel SGX hardware-software extension that aims to eliminate SGX-Step’s single-stepping capabilities by prefetching selected application pages. Notably, AEX-Notify is an *opt-in* feature that is only available in recent CPUs. With regards to our attacks, victim enclaves that opt-in to AEX-Notify would preclude the ability to gather precise instruction counts through single-stepping. However, AEX-Notify explicitly

does *not* prevent general information leakage through page faults and, hence, cannot fully mitigate our attacks.

8.2. Limitations

There are a certain limitations to our proof of concept.

We require the victim to run in a co-located TEE in order to use our controlled channel, which is a different requirement than previous model stealing attacks, which require chosen inputs and the output distribution of the inference pass.

Despite the recovery of the first layer of neurons fundamentally undermining SGX’s promise to secure the entire computation, our attack is limited in recovering parameters from deeper layers, depending on the model architecture. This is mostly due to the (limited) expressive power of some common activation functions as noted in Table 1 and detailed in Section 5.3. Besides, the used grid search is less efficient than binary search for the first layers, and depending on the magnitude of the weights, small search steps might be needed to discover thresholds. An adaptive approach could be used where the sweep region is deepened until a threshold is hit. We note however that small weights likely contribute little to the network, and thus could be replaced by a static value during the recovery process, producing an equivalent (though not identical) network.

8.3. Future Work

To efficiently recover missing parameters from deeper layers, if the output of the network is available, our attack could be combined with a Tramèr-style attack. After a partial parameter recovery, the obtained parameters would be placed into an untrained network with identical architecture, and be locked during training as in transfer learning. Then, the remaining neurons can be trained using examples generated from input/output pairs from the source network. In particular, image processing and similar networks contain a large proportion of their parameters in the early layers (and have an overall funnel shape), hence, this might result in a more precise recovery compared to a brute-force approach.

Besides, we demonstrated our attack approach for simple FNNs. It would be interesting to expanding the attack to more complex architectures like Convolutional Neural Networks (CNNs) or transformers, using a library OS like Gramine⁴ to run the relevant code in an SGX enclave. To improve the performance of our attack, a weighted binary search could reduce the number of search steps, as could caching some shared state such as the during the calibration step.

Finally, we focused on input-dependent memory access patterns and instruction counts in this paper, but did not take input-dependent latency of single instructions into account.

For example, the `UCOMISS` instruction discussed in Section 7.2.1 is not necessarily guaranteed to execute in constant time [26], and can raise floating point exceptions. This could render vectorised code like the implementation from `sleef` vulnerable to a modified version of

4. <https://github.com/gramineproject/gramine>

our attack: while different inputs might have identical instruction counts (as reported by SGX-Step), the actual runtime might be different and be observable with other side channels like IRQ latency [37].

9. Conclusion

The recent surge in ML applications necessitates an in-depth understanding of new types of attack vectors and defenses. In this respect, confidential computing architectures, and in particular Intel SGX, have gained significant traction in recent years and hold the potential to securely outsourcing critical ML computations to pervasive untrusted remote cloud platforms. This paper showed, however, that SGX-protected ML implementations exhibit subtle side-channel vulnerabilities that allow to extract precise model weight and biases in practical proof-of-concept attacks. In the wider perspective, our work may generalise to other TEEs and highlights the issue of input-dependent memory accesses that are prevalent in today's ML implementations, suggesting that security-critical ML applications should consider adopting coding practices studied in the cryptographic community.

Acknowledgments

The PhD of Jesse Spielman is partially funded by a donation from Intel. This research was further partially funded by the Engineering and Physical Sciences Research Council (EPSRC) under grants EP/X03738X/1 and EP/R012598/1. This research is partially funded by the Research Fund KU Leuven, and by the Cybersecurity Research Program Flanders.

References

- [1] M. Russinovich, "Confidential computing: Elevating cloud security and privacy," *Commun. ACM*, vol. 67, no. 1, 52–53, Dec. 2023.
- [2] Intel, *Reference Architecture for Privacy Preserving Machine Learning with Intel® SGX and Tensor-Flow*, en, 2024.
- [3] U. Kumar and E. Sakata, *Protecting Sensitive Data and AI Models with Confidential Computing*, <https://developer.nvidia.com/blog/protecting-sensitive-data-and-ai-models-with-confidential-computing/>, 2023.
- [4] Q. Li, Y. Xie, T. Du, *et al.*, "Coreguard: Safeguarding foundational capabilities of llms against model stealing in edge deployment," *arXiv preprint arXiv:2410.13903*, 2024.
- [5] R. R. Kethireddy, "Secure model distribution and deployment for llms," *Journal of Recent Trends in Computer Science and Engineering (JRTCSE)*, vol. 12, no. 4, pp. 1–14, 2024.
- [6] J. Van Bulck, F. Piessens, and R. Strackx, "SGX-Step: A Practical Attack Framework for Precise Enclave Execution Control," in *Proceedings of the 2nd Workshop on System Software for Trusted Execution*, ser. SysTEX'17, New York, NY, USA: Association for Computing Machinery, Oct. 2017, pp. 1–6, ISBN: 978-1-4503-5097-6.
- [7] F. Tramèr, F. Zhang, A. Juels, M. K. Reiter, and T. Ristenpart, "Stealing Machine Learning Models via Prediction APIs," *arXiv:1609.02943 [cs, stat]*, Oct. 2016, arXiv: 1609.02943 version: 2.
- [8] Intel, *Intel Software Guard Extensions Protects Data*, en, 2023.
- [9] A. Nilsson, P. N. Bideh, and J. Brorsson, *A Survey of Published Attacks on Intel SGX*, en, arXiv:2006.13598 [cs], Jun. 2020.
- [10] ARM, *TrustZone for Cortex-A*, 2024.
- [11] Intel, *Trust Domain Extensions (Intel TDX)*, 2024.
- [12] AMD, *AMD Secure Encrypted Virtualization (SEV)*, 2024.
- [13] I. A. Canales-Martínez, J. Chávez-Saab, A. Hambitzer, F. Rodríguez-Henríquez, N. Satpute, and A. Shamir, "Polynomial time cryptanalytic extraction of neural network models," in *Annual International Conference on the Theory and Applications of Cryptographic Techniques*, Springer, 2024, pp. 3–33.
- [14] M. Yan, C. W. Fletcher, and J. Torrellas, "Cache Telepathy: Leveraging Shared Resource Attacks to Learn {DNN} Architectures," en, 2020, pp. 2003–2020, ISBN: 978-1-939133-17-5.
- [15] S. Hong, M. Davinroy, Y. Kaya, *et al.*, *Security analysis of deep neural networks operating in the presence of cache side-channel attacks*, 2020. arXiv: 1810.03487 [cs.CR].
- [16] V. Duddu, D. Samanta, D. V. Rao, and V. E. Balas, *Stealing neural networks via timing side channels*, 2019. arXiv: 1812.11720 [cs.CR].
- [17] Y.-S. Won, S. Chatterjee, D. Jap, S. Bhasin, and A. Basu, "Time to leak: Cross-device timing attack on edge deep learning accelerator," in *2021 International Conference on Electronics, Information, and Communication (ICEIC)*, 2021, pp. 1–4. DOI: 10.1109/ICEIC51217.2021.9369754.
- [18] H. Naghibijouybari, A. Neupane, Z. Qian, and N. Abu-Ghazaleh, "Rendered Insecure: GPU Side Channel Attacks are Practical," in *Proceedings of the 2018 ACM SIGSAC Conference on Computer and Communications Security*, ser. CCS '18, Toronto, Canada: Association for Computing Machinery, 2018, 2139–2153, ISBN: 9781450356930. DOI: 10.1145/3243734.3243831. [Online]. Available: <https://doi.org/10.1145/3243734.3243831>.
- [19] J. Wei, Y. Zhang, Z. Zhou, Z. Li, and M. A. Al Faruque, "Leaky DNN: Stealing Deep-Learning Model Secret with GPU Context-Switching Side-Channel," in *2020 50th Annual IEEE/IFIP International Conference on Dependable Systems and Networks (DSN)*, 2020, pp. 125–137. DOI: 10.1109/DSN48063.2020.00031.
- [20] H. Naghibijouybari, A. Neupane, Z. Qian, and N. Abu-Ghazaleh, "Side Channel Attacks on GPUs," *IEEE Transactions on Dependable and Secure Computing*, vol. 18, no. 4, pp. 1950–1961, 2021. DOI: 10.1109/TDSC.2019.2944624.
- [21] G. Dong, P. Wang, P. Chen, R. Gu, and H. Hu, "Floating-point multiplication timing attack on deep neural network," in *2019 IEEE International Conference on Smart Internet of Things (SmartIoT)*,

- 2019, pp. 155–161. DOI: 10.1109/SmartIoT.2019.00032.
- [22] R. S. Ali, B. Z. H. Zhao, H. J. Asghar, T. Nguyen, I. D. Wood, and D. Kaafar, *Unintended memorization and timing attacks in named entity recognition models*, 2022. arXiv: 2211.02245 [cs.CR].
- [23] T. Nakai, D. Suzuki, and T. Fujino, “Timing black-box attacks: Crafting adversarial examples through timing leaks against dnns on embedded devices,” *IACR Transactions on Cryptographic Hardware and Embedded Systems*, vol. 2021, no. 3, 149–175, Jul. 2021. DOI: 10.46586/tches.v2021.i3.149-175. [Online]. Available: <https://tches.iacr.org/index.php/TCHES/article/view/8971>.
- [24] Y. Dan, T. Shibahara, and J. Takahashi, “Timing attack on random forests: Experimental evaluation and detailed analysis,” *Journal of Information Processing*, vol. 29, pp. 757–768, 2021. DOI: 10.2197/ipsjip.29.757.
- [25] F. Alder, J. Van Bulck, D. Oswald, and F. Piessens, “Faulty Point Unit: ABI Poisoning Attacks on Intel SGX,” in *Proceedings of the 36th Annual Computer Security Applications Conference*, ser. ACSAC ’20, Austin, USA: Association for Computing Machinery, 2020, 415–427, ISBN: 9781450388580. DOI: 10.1145/3427228.3427270. [Online]. Available: <https://doi.org/10.1145/3427228.3427270>.
- [26] C. Gongye, Y. Fei, and T. Wahl, “Reverse-engineering deep neural networks using floating-point timing side-channels,” in *Proceedings of the 57th ACM/EDAC/IEEE Design Automation Conference*, ser. DAC ’20, Virtual Event, USA: IEEE Press, 2020, ISBN: 9781450367257.
- [27] W. Hua, Z. Zhang, and G. E. Suh, “Reverse engineering convolutional neural networks through side-channel information leaks,” in *2018 55th ACM/ESDA/IEEE Design Automation Conference (DAC)*, 2018, pp. 1–6. DOI: 10.1109/DAC.2018.8465773.
- [28] L. Batina, S. Bhasin, D. Jap, and S. Picek, “CSI NN: Reverse engineering of neural network architectures through electromagnetic side channel,” in *28th USENIX Security Symposium (USENIX Security 19)*, Santa Clara, CA: USENIX Association, Aug. 2019, pp. 515–532, ISBN: 978-1-939133-06-9. [Online]. Available: <https://www.usenix.org/conference/usenixsecurity19/presentation/batina>.
- [29] H. Yu, H. Ma, K. Yang, Y. Zhao, and Y. Jin, “DeepEM: Deep Neural Networks Model Recovery through EM Side-Channel Information Leakage,” in *2020 IEEE International Symposium on Hardware Oriented Security and Trust (HOST)*, 2020, pp. 209–218. DOI: 10.1109/HOST45689.2020.9300274.
- [30] P. Horvath, L. Chmielewski, L. Weissbart, L. Batina, and Y. Yarom, *BarraCUDA: GPUs do Leak DNN Weights*, 2024. arXiv: 2312.07783 [cs.CR].
- [31] W. Wang, G. Chen, X. Pan, *et al.*, “Leaky Cauldron on the Dark Land: Understanding Memory Side-Channel Hazards in SGX,” in *Proceedings of the 2017 ACM SIGSAC Conference on Computer and Communications Security*, ser. CCS ’17, Dallas, Texas, USA: Association for Computing Machinery, 2017, 2421–2434, ISBN: 9781450349468.
- [32] F. Brasser, U. Müller, A. Dmitrienko, K. Kostinainen, S. Capkun, and A.-R. Sadeghi, “Software grand exposure: SGX cache attacks are practical,” in *11th USENIX Workshop on Offensive Technologies (WOOT 17)*, Vancouver, BC: USENIX Association, Aug. 2017.
- [33] Y. Xu, W. Cui, and M. Peinado, “Controlled-Channel Attacks: Deterministic Side Channels for Untrusted Operating Systems,” en, in *2015 IEEE Symposium on Security and Privacy*, San Jose, CA: IEEE, May 2015, pp. 640–656, ISBN: 978-1-4673-6949-7.
- [34] S. Shinde, Z. L. Chua, V. Narayanan, and P. Saxena, “Preventing page faults from telling your secrets,” in *11th ACM Asia Conference on Computer and Communications Security (AsiaCCS)*, 2016, pp. 317–328.
- [35] J. Van Bulck, N. Weichbrodt, R. Kapitza, F. Piessens, and R. Strackx, “Telling your secrets without page faults: Stealthy page table-based attacks on enclaved execution,” in *26th USENIX Security Symposium*, Aug. 2017, pp. 1041–1056.
- [36] J. Van Bulck and F. Piessens, “SGX-Step: An open-source framework for precise dissection and practical exploitation of Intel SGX enclaves,” in *ACSAC 2023 Cybersecurity Artifacts Competition and Impact Award Finalist Short Paper*, Dec. 2023.
- [37] J. Van Bulck, F. Piessens, and R. Strackx, “Nemesis: Studying Microarchitectural Timing Leaks in Rudimentary CPU Interrupt Logic,” in *Proceedings of the 2018 ACM SIGSAC Conference on Computer and Communications Security*, ser. CCS ’18, Toronto, Canada: Association for Computing Machinery, 2018, 178–195, ISBN: 9781450356930. DOI: 10.1145/3243734.3243822. [Online]. Available: <https://doi.org/10.1145/3243734.3243822>.
- [38] D. Moghimi, J. Van Bulck, N. Heninger, F. Piessens, and B. Sunar, “CopyCat: Controlled instruction-level attacks on enclaves,” in *29th USENIX Security Symposium*, Aug. 2020, pp. 469–486.
- [39] A. C. Aldaya and B. B. Brumley, “When one vulnerable primitive turns viral: Novel single-trace attacks on ECDSA and RSA,” *IACR Transactions on Cryptographic Hardware and Embedded Systems*, pp. 196–221, 2020.
- [40] J. Van Bulck, D. Oswald, E. Marin, A. Aldoseri, F. D. Garcia, and F. Piessens, “A Tale of Two Worlds: Assessing the Vulnerability of Enclave Shielding Runtimes,” en, in *Proceedings of the 2019 ACM SIGSAC Conference on Computer and Communications Security*, London United Kingdom: ACM, Nov. 2019, pp. 1741–1758, ISBN: 978-1-4503-6747-9.
- [41] S. Constable, J. Van Bulck, X. Cheng, *et al.*, “AEX-Notify: Thwarting precise single-stepping attacks through interrupt awareness for Intel SGX enclaves,” in *32nd USENIX Security Symposium*, Aug. 2023, pp. 4051–4068.
- [42] I. Puddu, M. Schneider, D. Lain, S. Boschetto, and S. Čapkun, “On (the lack of) code confidentiality

- in trusted execution environments,” in *2024 IEEE Symposium on Security and Privacy (SP)*, IEEE, 2024, pp. 4125–4142.
- [43] M. Choi, *Medical cost personal datasets*, 2018.
- [44] Sun Microsystems, *Tlibc’s expf implementation*, https://github.com/intel/linux-sgx/blob/80a662/sdk/tlibc/math/e_expf.c, 1993.
- [45] D. Kohlbrenner and H. Shacham, “On the effectiveness of mitigations against floating-point timing channels,” in *26th USENIX Security Symposium (USENIX Security 17)*, Vancouver, BC: USENIX Association, Aug. 2017, pp. 69–81, ISBN: 978-1-931971-40-9. [Online]. Available: <https://www.usenix.org/conference/usenixsecurity17/technical-sessions/presentation/kohlbrenner>.
- [46] L. Wilke, J. Wichelmann, A. Rabich, and T. Eisenbarth, “SEV-Step A Single-Stepping Framework for AMD-SEV,” *IACR Transactions on Cryptographic Hardware and Embedded Systems*, vol. 2024, no. 1, pp. 180–206, Dec. 2023. DOI: 10.46586/tches.v2024.i1.180-206. [Online]. Available: <https://tches.iacr.org/index.php/TCHES/article/view/11250>.
- [47] L. Wilke, F. Sieck, and T. Eisenbarth, “TDXdown: Single-stepping and instruction counting attacks against intel TDX,” in *Proceedings of the 2024 ACM SIGSAC Conference on Computer and Communications Security, CCS 2024, Salt Lake City, UT, USA, October 14–18, 2024*, 2024. DOI: 10.1145/3658644.3690230.
- [48] P. Shome, *Closing the Intel TDX page fault side channel, or, the case for TDExit-Notify*, <https://collective.flashbots.net/t/closing-the-intel-tdx-page-fault-side-channel-or-the-case-for-tdexit-notify/3775/1>, Aug. 2024.
- [49] A. Purnal, F. Turan, and I. Verbauwhede, “Prime+Scope: Overcoming the Observer Effect for High-Precision Cache Contention Attacks,” in *Proceedings of the 2021 ACM SIGSAC Conference on Computer and Communications Security*, ser. CCS ’21, Virtual Event, Republic of Korea: Association for Computing Machinery, 2021, pp. 2906–2920, ISBN: 9781450384544. DOI: 10.1145/3460120.3484816. [Online]. Available: <https://doi.org/10.1145/3460120.3484816>.
- [50] M.-W. Shih, S. Lee, T. Kim, and M. Peinado, “T-SGX: Eradicating Controlled-Channel Attacks Against Enclave Programs,” in *24th Annual Network and Distributed System Security Symposium (NDSS)*, Feb. 2017.
- [51] S. ul Hassan, I. Gridin, I. M. Delgado-Lozano, et al., “Déjà vu: Side-channel analysis of mozilla’s nss,” *arXiv preprint arXiv:2008.06004*, 2020.
- [52] O. Oleksenko, B. Trach, R. Krahn, M. Silberstein, and C. Fetzer, “Varys: Protecting SGX enclaves from practical side-channel attacks,” in *USENIX Annual Technical Conference (ATC)*, 2018, pp. 227–240.
- [53] S. Aga and S. Narayanasamy, “Invisipage: Oblivious demand paging for secure enclaves,” in *Proceedings of the 46th International Symposium on Computer Architecture*, 2019, pp. 372–384.
- [54] P. Zhang, C. Song, H. Yin, D. Zou, E. Shi, and H. Jin, “Klotski: Efficient obfuscated execution against controlled-channel attacks,” in *Proceedings of the Twenty-Fifth International Conference on Architectural Support for Programming Languages and Operating Systems*, 2020, pp. 1263–1276.
- [55] F. Brasser, S. Capkun, A. Dmitrienko, T. Frassetto, K. Kostianen, and A.-R. Sadeghi, “Dr. SGX: automated and adjustable side-channel protection for SGX using data location randomization,” in *35th Annual Computer Security Applications Conference (ACSAC)*, 2019, pp. 788–800.

Appendix A. Example Attack Output

```

1 [ Neuron 2 ]
2 stats:
3   952.99 seconds since start
4   1439 executions so far
5   4 Incomplete logs
6   0 non-deterministic steps
7   6 neuron_check failures
8 Function = exp
9 Search strategy: seeded binary search
10  Calibrating:
11     count: 14
12     recovered signs: + - - - + - - - + +
13     recovered maxvals: 1000 1000 1000 1000 1000 1000 1000 10000
14     1000 1000 10000 10000 1000
15 Finding convergence points for equation 1
16 depth 0: Overflow
17 depth 10: Normal
18 depth 20: Overflow
19 depth 30: Normal
20 depth 40: Overflow
21 depth 50: Overflow
22 Finding convergence points for equation 2
23 <SNIP>
24 Finding convergence points for equation 12
25 depth 0: Overflow
26 depth 10: Normal
27 depth 20: Normal
28 depth 30: Normal
29 depth 40: Overflow
30 depth 50: Overflow
31 deepest solution: [
32   0.14825567 -0.17573831 -0.28457861 -0.24754734
33   0.09355622 -0.09359772 -0.2866397 -0.2083804
34   -0.10068617 0.07542896 0.10219476 -0.04099777]
35 ground truth: [
36   0.14825566 -0.17573832 -0.28457862 -0.24754737
37   0.09355621 -0.09359772 -0.28663969 -0.2083804
38   -0.10068618 0.07542896 0.10219476 -0.04099637]
39 abs percent error: [
40   0.0%, 0.0%, 0.0%, 0.0%, 0.0%, 0.0%, 0.0%, 0.0%,
41   0.0%, 0.0%, 0.0%, 0.0%, 0.0%, 0.0%, 0.0%, 0.0%]
42 Checkpoint saved!

```

Listing 6. Example output from our attack tool finding convergence points.

Appendix B. Implementation of sigmoid() (called logistic()) in Tensorflow lite

```

1 inline void Logistic(const RuntimeShape& input_shape,
2   const float* input_data,
3   const RuntimeShape& output_shape,
4   float* output_data) {
5   const float cutoff_upper = 16.619047164916992188f;
6   const float cutoff_lower = -9.f;
7
8   const int flat_size = MatchingFlatSize(input_shape,
9   output_shape);
10
11  // [comments removed]
12
13  for (int i = 0; i < flat_size; i++) {
14    float val = input_data[i];
15    float result;
16    if (val > cutoff_upper) {
17      result = 1.0f;
18    } else if (val < cutoff_lower) {
19      result = std::exp(val);
20    } else {
21      result = 1.f / (1.f + std::exp(-val));
22    }
23    output_data[i] = result;
24  }
25 }

```

Listing 7. Implementation of Logistic() in Tensorflow lite

Appendix C. Error Comparison with Extra Convergence Sets

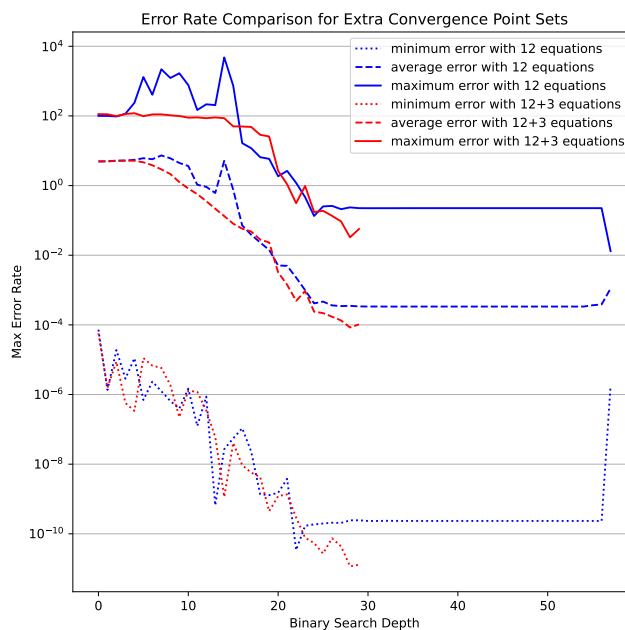


Figure 5. Note the effect that extra convergence sets have to reduce variance and lessen the errors, especially after depth=25